Electron-hole pairing in a topological insulator thin film

D. K. Efimkin,[1] Yu. E. Lozovik,[1,2,*] and A. A. Sokolik[1,†]

[1]*Institute for Spectroscopy, Russian Academy of Sciences, RU-142190 Troitsk, Moscow Region, Russia*

[2]*Moscow Institute of Physics and Technology, RU-141700 Dolgoprudny, Moscow Region, Russia*

(Received 7 July 2012; revised manuscript received 1 September 2012; published 21 September 2012)

We consider the pairing of massless Dirac electrons and holes located on opposite surfaces of thin films of "strong" three-dimensional topological insulators. Such pairing is predicted to give rise to a topological exciton condensate with unusual properties. We estimate the quantitatively achievable critical temperature of the pairing while taking into account the self-consistent screening of the Coulomb interaction, disorder, and hybridization of electron and hole states caused by tunneling through the film. The increase of the gap above the hybridization value when the temperature is lowered can be an observable signature of the pairing. System parameters required to observe the electron-hole pairing are discussed.

DOI: 10.1103/PhysRevB.86.115436 PACS number(s): 71.35.−y, 73.20.−r, 73.22.Gk

I. INTRODUCTION

The research of nontrivial topological states of matter has been highly stimulated in recent years by the discovery of two- and three-dimensional topological insulators (TIs).[1,2] Nonzero topological invariant characterizing global topology of filled electron states in Hilbert space across the whole Brillouin zone distinguishes a TI from a trivial insulator. One of the most interesting properties of TIs is the existence of gapless, topologically protected edge (in a two-dimensional case) or surface (in a three-dimensional case) electron states.

Unusual properties of surface modes manifest themselves most strikingly in the second generation of "strong" three-dimensional TIs represented by such materials as Bi_2Se_3, Bi_2Te_3, Sb_2Te_3, Bi_2Te_2Se, and others.[3–6] In these materials, the band structures of the surface states contain a Dirac cone, and electrons obey a two-dimensional Dirac-Weyl equation for massless particles in the vicinity of a Dirac point. Electrons in graphene demonstrate similar properties but have two inequivalent Dirac cones and additional twofold degeneracy by spin projections.[7]

A gap in the spectrum of a surface states can be induced when the time-reversal symmetry is broken by magnetic impurities or in the proximity of a ferromagnet.[8–10] When the gap is opened in such a way on the whole surface of a TI, a spectacular topological magnetoelectric effect arises.[10,11] Another way to open the gap is to break the gauge symmetry by contact with a superconductor at which point the surface of the TI acquires the properties of a topological superconductor.[12] Intrinsic Cooper pairing involving surface Dirac electrons induced by some mechanism can also lead to an analog of topological superconductivity on the surface of a TI.[13–15]

Such strong three-dimensional TIs as Bi_2Se_3, Bi_2Te_3, etc. have layered crystal structures[3,5] with each layer consisting of five atomic layers [a quintuple layer (QL)] and having a thickness of about 1 nm. The fabrication of thin films of these materials with arbitrary thicknesses, down to only 1 QL, was realized recently by means of epitaxial methods,[16–19] by vapor-solid growth,[20] and by mechanical exfoliation.[21–23] Electronic properties of TI thin films are strongly affected by tunneling between opposite surfaces, which gives rise to a hybridization gap[18,24–29] and other observable phenomena, for example, unusual spin arrangements and splitting of the zero-energy Landau level.[30–33]

Chiral electrons on opposite surfaces of a TI film constitute a strongly coupled bilayer system which, in principle, can demonstrate various coherent quantum phenomena. In the case of antisymmetric doping of these surfaces, one can realize a Coulomb-interaction-mediated pairing of electrons on one surface of the film and holes on the opposite surface,[34–43] similar to the pairing proposed earlier for massive electrons and holes in coupled semiconductor quantum wells[44–47] and for massless Dirac electrons and holes in a graphene bilayer.[48–58] This kind of pairing is similar to the Cooper pairing of electrons in superconductors but occurs between spatially separated electrons and holes.

Although graphene, owing to its monoatomic thickness, allows the fabrication of two-layer structures with record small interlayer distances and demonstrates high carrier mobilities,[7] the fourfold degeneracy of its electron states leads to very strong screening of the pairing interaction and thus to rather low critical temperatures.[53,55] In the case of TI films, predictions for the critical temperature of the pairing can be much more optimistic since electron states there have no degeneracy as noted in Refs. 34, 36, and 41.

Besides the weaker screening, the pairing in TI films could be more interesting from the viewpoint of the superfluid properties of the resulting topological "exciton" condensate. Zero-energy Majorana modes bound to vortex cores, gapless states on a contact with superconductor and other interesting phenomena, were predicted in such systems.[34–36,42] However, whether the electron-hole pairing is achievable in TI films in practice is not yet known. A critical temperature for the superfluid state of about 100 K was estimated in Ref. 38, however, without taking into account the screening. In approximation of the separable potential, critical temperatures up to 0.1 K were obtained.[39] The recent, more complicated calculations including dynamical screening and correlation effects resulted in rather optimistic estimates (about 100–200 K) for the zero-temperature gap.[41] For the quantum Hall regime, gaps on the order of hundreds of Kelvins were predicted.[37]

In our article, we study observable signatures of the electron-hole pairing in TI films in realistic conditions, taking into account interaction screening, hybridization, and disorder.

We start with descriptions of the pairing in a simple Bardeen-Cooper-Schrieffer (BCS) approximation (Sec. II) and show that the critical temperature takes practically observable values (at least 0.1 K) only at film thicknesses less than 15 nm. Hybridization between opposite surfaces significantly affects the pairing at such small thicknesses as studied in Sec. III. Detection of the pairing against a background of strong hybridization becomes the major issue here. We show that the increase of the gap due to the pairing as the temperature is lowered can be observed in TI films of moderate thicknesses of about 5–8 QLs.

Our study of the suppression of the pairing by disorder in Sec. IV shows that the pairing requires rather high carrier mobilities to be observable. In Sec. V, we demonstrate that the screening in a system with an induced gap is suppressed in comparison with the metalliclike screening assumed in the previous sections. By taking into account this correlation effect, we find out that the predicted gap greatly increases in moderately thin films.

The calculations in this article refer to the case of Bi_2Se_3 films with a 0.96-nm thickness of 1 QL.[19] However, our conclusions can be extended to other TIs of similar types with controlling parameters (Fermi velocity, dielectric permittivity, and hybridization gaps) similar to those of Bi_2Se_3.

II. BCS APPROXIMATION

One of the possible setups for the pairing is depicted in Fig. 1. The opposite electric potentials $\pm V$ imposed on the opposite surfaces of the TI film either by gate electrodes or by appropriate contacts cause antisymmetric doping of these surfaces with electrons (top surfaces) and holes (bottom surface) up to the chemical potentials μ and $-\mu$, respectively (Fig. 2). For simplicity, we assume here electron-hole symmetry. An alternative method to create electrons and holes can be based on the chemical doping of the surfaces.

The inverted structure "TI-insulator-TI" was also proposed by several authors,[35,36,38,42] but we shall demonstrate below that it is less suitable for the pairing.

The Coulomb interaction between the electron and hole residing on opposite surfaces of a TI film undergoes combined screening by a three-dimensional dielectric environment and by a two-dimensional electron and hole gas on these surfaces. We consider the three-layer dielectric system (Fig. 1) where

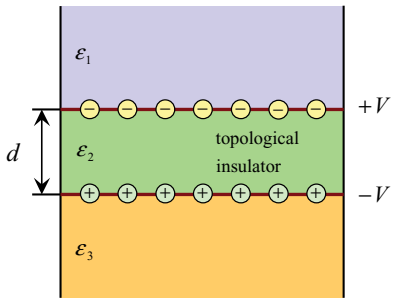

FIG. 1. (Color online) TI film of thickness d and dielectric permittivity ε_2 surrounded by trivial insulators with permittivities ε_1 and ε_3. Electric potentials $\pm V$ on opposite surfaces of the film create electron and hole gases of equal concentrations.

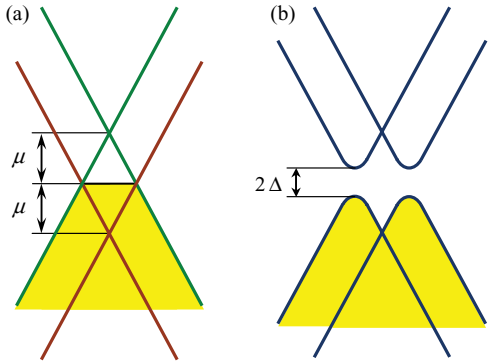

FIG. 2. (Color online) Band picture of the pairing. (a) The applied potential difference shifts energies of Dirac cones on opposite surfaces in opposite directions in such a way that electron and hole gases with chemical potentials μ and $-\mu$ are formed. (b) The pairing opens a gap 2Δ on the Fermi level.

ε_2 is the dielectric permittivity of the TI film and ε_1 and ε_3 are dielectric permittivities of insulators above and below the film, respectively. In such a system, the statically screened electron-hole interaction in the random-phase approximation (RPA) is $-V(q)$, where

$$V(q)=\frac{4\pi e^2}{qD(q)}\left[\varepsilon_2+\frac{4\pi e^2}{q}\Pi_{12}(q)\sinh(qd)\right] \tag{1}$$

(see also the similar formulas in Refs. 37 and 44). Here,

$$\begin{aligned}D(q)=&\left(\varepsilon_1\varepsilon_3+\varepsilon_2^2\right)\sinh(qd)+(\varepsilon_1+\varepsilon_3)\varepsilon_2\cosh(qd)\\&-\frac{4\pi e^2}{q}[S_{11}(q)\Pi_{11}(q)+S_{22}(q)\Pi_{22}(q)+2\varepsilon_2\Pi_{12}(q)]\\&+\frac{16\pi^2e^4}{q^2}\left[\Pi_{11}(q)\Pi_{22}(q)-\Pi_{12}^2(q)\right]\sinh(qd),\end{aligned} \tag{2}$$

where

$$\begin{aligned}S_{11}(q)&=\varepsilon_3\sinh(qd)+\varepsilon_2\cosh(qd),\\S_{22}(q)&=\varepsilon_1\sinh(qd)+\varepsilon_2\cosh(qd),\end{aligned} \tag{3}$$

and where $\Pi_{11}(q)$ and $\Pi_{22}(q)$ are static polarizabilities of electron and hole gases on the top and bottom surfaces of the film, respectively; $\Pi_{12}(q)$ is the static anomalous interlayer polarizability; and d is the thickness of the film.

We shall consider the pairing in the static approximation, i.e., by neglecting frequency dependencies of the gap and pairing potential. At $0\leqslant q\leqslant 2p_F$, the static polarizability of a Dirac electron or hole gas is $\Pi_0(q)=-g\mathcal{N}$,[59,60] where g is the degeneracy factor, $\mathcal{N}=\mu/2\pi v_F^2$ is the density of states at the Fermi level, $p_F=\mu/v_F$ is the Fermi momentum, and v_F is the Fermi velocity of Dirac electrons and holes (6.2×10^5 m/s for Bi_2Se_3).[3]

In this section, we assume that the screening is the same as in an intrinsic system without pairing, setting $\Pi_{11}=\Pi_{22}=\Pi_0$ and $\Pi_{12}=0$. The main advantage of a TI film over a graphene bilayer is the smaller degeneracy factor $g=1$ (vs $g=4$ for graphene), providing a weaker screening.

The static dielectric permittivity of strong three-dimensional TIs is rather large [e.g., $\varepsilon_2\approx80$ for Bi_2Se_3 (Ref. 61) and $\varepsilon_2\approx30$ for Bi_2Te_3 (Ref. 62)], which looks disappointing for the realization of the pairing. However, when

the thickness of the film d is much smaller than the mean in-plane distance between electrons and holes (on the order of p_F^{-1}), electric-field lines responsible for the electron-hole interaction pass mainly through the media above and below the film. In this case the screening is the same as in a homogeneous medium with the dielectric permittivity $(\varepsilon_1+\varepsilon_3)/2$ and does not depend on the dielectric permittivity ε_2 of the film itself. [It follows directly from the limit $qd \ll 1$ of Eqs. (1)–(3) and was also noted in Ref. 37.]

Generally, the pairing of massless Dirac fermions can be multiband when both the valence and conduction bands of both layers are affected by the pairing correlations. The multiband theory of the pairing in a graphene bilayer provides larger estimates for the gap and critical temperature than the usual one-band BCS model both in static and dynamic approximations.[54–56] For the sake of simplicity, here we shall consider the pairing in the one-band BCS model, being aware, however, that our results for the gap and critical temperature can be underestimated.

The integral BCS equation for the gap function $\Delta(\mathbf{p})$ in the one-band approximation is as follows (analogous to that in Refs. 49 and 54):

$$\Delta(\mathbf{p}) = \int \frac{d\mathbf{p}'}{(2\pi)^2} \frac{1+\cos(\varphi-\varphi')}{2} V(|\mathbf{p}-\mathbf{p}'|) \times \left[\frac{\Delta(\mathbf{p}')}{2E(\mathbf{p}')} \tanh\frac{E(\mathbf{p}')}{2T}\right], \tag{4}$$

where φ and φ' are azimuthal angles of the momenta $\mathbf{p}$ and $\mathbf{p}'$, respectively, entering the angular factor, specific to chiral Dirac electrons; $E(\mathbf{p}) = \sqrt{(v_F p-\mu)^2 + |\Delta(\mathbf{p})|^2}$ is the Bogolyubov excitation energy; and T is the temperature.

According to the usual BCS recipe, we assume that the gap is nonzero and constant in some energy region of the half-width w around the Fermi surface:

$$\Delta(\mathbf{p}) = \begin{cases} \Delta, & \text{if} \quad |v_F p-\mu| \leqslant w, \\ 0, & \text{if} \quad |v_F p-\mu| > w. \end{cases} \tag{5}$$

Using Eqs. (4) and (5), we can find the gap at $T=0$

$$\Delta_0^{\mathrm{BCS}} = 2we^{-1/\lambda} \tag{6}$$

and the critical temperature

$$T_c = \frac{2we^{\gamma}}{\pi} e^{-1/\lambda}. \tag{7}$$

Here, $\gamma \approx 0.577$ is the Euler constant, and λ is the dimensionless coupling constant calculated as an average of the interaction potential times the density of states over the Fermi surface:

$$\lambda = \int_0^{2\pi} \frac{d\varphi}{2\pi} \frac{1+\cos\varphi}{2} \mathcal{N} V\left(2p_F \sin\frac{\varphi}{2}\right). \tag{8}$$

It is reasonable to take the pairing region half-width w on the order of the chemical potential μ since there are no other energy scales in the system (in contrast to superconductors in which w can be taken on the order of the Debye frequency). Thus, hereafter we take $w=\mu$. The maximal level of surface doping relative to the Dirac point in the present three-dimensional TIs, being limited by the position of the bulk valence band, is about $\mu \approx 0.1$ eV.[3] If we assume that the critical temperature of Eq. (7) should be at least 0.1 K for the pairing to be observable, then at the maximal $w=\mu=0.1$ eV, the coupling constant λ should not be less than 0.14.

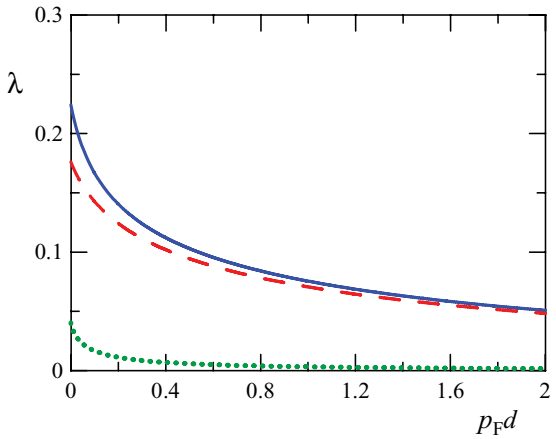

FIG. 3. (Color online) The coupling constant of Eq. (8) for the pairing in a Bi_2Se_3 film with $\varepsilon_2=80$ as a function of $p_F d$ at $\varepsilon_1=\varepsilon_3=1$ (solid line), at $\varepsilon_1=\varepsilon_3=4$ (dashed line), and for the TI-vacuum-TI system with $\varepsilon_1=\varepsilon_3=80$ and $\varepsilon_2=1$ (dotted line).

The coupling constants in the cases of a suspended Bi_2Se_3 film with $\varepsilon_1=\varepsilon_3=1$ and of a film surrounded by a dielectric with $\varepsilon_1=\varepsilon_3=4$ are plotted in Fig. 3 at various $p_F d$. It is seen that in both cases λ falls off very rapidly with increasing $p_F d$, and $\lambda > 0.14$ requires $p_F d < 0.2$. We see also that strong screening by bulk TIs significantly suppresses the coupling constant in the inverted structure TI-insulator-TI even in the most favorable case of a vacuum spacer with $\varepsilon_2=1$.

We can bring the coupling constant to its maximal value by approaching μ to zero and making the value of $p_F d$ arbitrarily small. However, the pre-exponential factor in Eq. (7), proportional to μ, also decreases in this case; in the limit $\mu \to 0$, the critical temperature in our approach tends to zero: $\Delta_0^{\mathrm{BCS}}, T_c \to 0$. Thus, we should not take too small a value for μ in order to reach the highest T_c. In Fig. 4 we plot T_c in a suspended Bi_2Se_3 film with $\varepsilon_1=\varepsilon_3=1$ as a function of μ at different thicknesses of d. It is seen that T_c is maximal at some nonzero μ dependent on d. In order to keep T_c above 0.1 K, we should take a film thickness d not exceeding 15 nm. A similar conclusion was made in Ref. 39. However, in this case, tunneling between electron states on opposite surfaces of the film leads to significant hybridization of the electron and hole states, which will be considered in the next section.

III. INFLUENCE OF HYBRIDIZATION

Wave functions of gapless electron states on the surface of a strong three-dimensional TI decay exponentially in the bulk with characteristic depth on the order of several nanometers.[29,30] In sufficiently thin films, the overlap of the wave functions of the states belonging to opposite surfaces of the film can occur. This results in the avoided crossing of dispersions of these states manifesting itself as the opening of the hybridization gap Δ_T. This gap in the spectrum is rather similar to the gap which could be opened by the pairing (see Fig. 2).

Indeed, the order parameter of the electron-hole pairing is $\langle a_{\mathbf{p}}^{(1)} b_{-\mathbf{p}}^{(2)} \rangle$, where $a_{\mathbf{p}}^{(1)}$ is the destruction operator for an electron

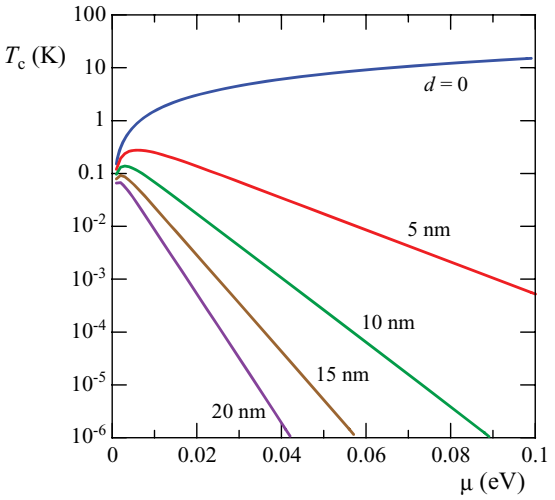

FIG. 4. (Color online) The BCS critical temperature of the pairing of Eq. (7) in a suspended Bi_2Se_3 film as a function of the chemical potential μ at different film thicknesses d, indicated near the corresponding curves.

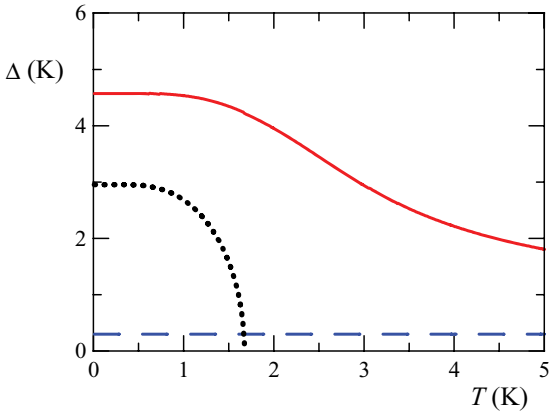

FIG. 5. (Color online) Conceptual example of the behavior of the gap Δ (solid line) as a function of temperature T in a system with hybridization at $\mu = 0.1$ eV, $\lambda = 0.15$, and $\Delta_T = 0.3$ K. The initial hybridization gap Δ_T (dashed line) and the BCS gap calculated without hybridization (dotted line) are shown for comparison.

with momentum $\mathbf{p}$ on the top surface and $b^{(2)}_{-\mathbf{p}}$ is the destruction operator for a hole with the opposite momentum $-\mathbf{p}$ on the bottom surface. Electron-hole transformation implies that $b^{(2)}_{-\mathbf{p}} = a^{(2)\dagger}_{\mathbf{p}}$, where $a^{(2)\dagger}_{\mathbf{p}}$ is the creation operator for an electron with momentum $\mathbf{p}$ on the bottom surface.

Therefore, the pair of operators entering the order parameter $\langle a^{(1)}_{\mathbf{p}} b^{(2)}_{-\mathbf{p}}\rangle = \langle a^{(1)}_{\mathbf{p}} a^{(2)\dagger}_{\mathbf{p}}\rangle$ is analogous to that describing the process of momentum-conserving electron tunneling between the top and bottom surfaces. Thus, the gap equation for the total energy gap in the mean-field approximation, describing both the pairing and hybridization, differs from Eq. (4) by the additional term Δ_T on the right-hand side:

$$\Delta(\mathbf{p}) = \Delta_T + \int \frac{d\mathbf{p}'}{(2\pi)^2} \frac{1+\cos(\varphi-\varphi')}{2} V(|\mathbf{p}-\mathbf{p}'|) \times \left[\frac{\Delta(\mathbf{p}')}{2E(\mathbf{p}')} \tanh\frac{E(\mathbf{p}')}{2T}\right]. \quad (9)$$

It is seen from Eq. (9) that the total gap Δ becomes larger than the hybridization gap Δ_T due to the pairing. We shall solve Eq. (9) similarly to Eq. (4) in the BCS-like approximation (5).

It should be noted that the interplay of pairing and hybridization was considered earlier for the case of the Bernal-stacked graphene bilayer in Ref. 48. In that case, interlayer tunneling and short-range interaction, being selective in different ways with respect to sublattices, led to gap equations of a more complicated form than Eq. (9).

In Fig. 5 the example of solution of Eq. (9) is plotted under conditions when the hybridization gap Δ_T is approximately ten times smaller than the zero-temperature BCS gap Δ_0^{BCS} calculated without hybridization. In the absence of hybridization, the gap Δ would vanish at some critical temperature, but nonzero hybridization makes Δ always nonzero and larger than Δ_T. At $T = 0$, the total gap is drastically increased even by weak hybridization; due to the nonlinearity of Eq. (9), it is larger than just a sum $\Delta_T + \Delta_0^{\mathrm{BCS}}$. At $T \to \infty$, the gap gradually tends to Δ_T. Thus, hybridization leads to the smearing of a phase transition into the paired state in close analogy with the behavior of a ferromagnet in an external magnetic field.

How can we observe the pairing in the presence of hybridization? Besides possible superfluid signatures of the pairing (see Sec. VI), we can still detect an increase of the gap in the spectrum when the temperature is lowered—from the pure hybridization value Δ_T at high temperatures to a somewhat larger value Δ_0 at zero (or very low) temperature (Fig. 5). To be observable, this increase should be relatively large, i.e., $\Delta_0 - \Delta_T$ should not be very small in comparison with Δ_T. In addition, the increase of the gap should occur in a reasonably narrow temperature range. This range can be estimated by a characteristic temperature T_{char} at which the gap is halfway between Δ_T and Δ_0, i.e., $\Delta(T_{\mathrm{char}}) - \Delta_T = [\Delta_0 - \Delta_T]/2$.

For calculations we take the data on the hybridization gaps in Bi_2Se_3 films from the experiment[25] in which the film thickness d ranges from 2 to 5 QLs and from the theoretical paper[29] in which d ranges from 1 to 16 QLs. (The close results for Δ_T were also presented in an earlier paper.[24]) It should be noted that in the overlapping region of d from 2 to 5 QLs, the experimental gaps from Ref. 25 are several times larger than the calculated gaps from Ref. 29, probably due to some impurities enhancing the interlayer tunneling.

According to these data, we take several examples of Bi_2Se_3 films with different d and Δ_T values. We take $\Delta_T = 0.126$ eV at $d = 2$ QLs and $\Delta_T = 0.02$ eV at $d = 5$ QLs from Ref. 25 as examples of large hybridization gaps (keeping in mind that the actual gap in the spectrum reported in the literature is $2\Delta_T$). As examples of small gaps, $\Delta_T = 6 \times 10^{-4}$ eV at $d = 5$ QLs and $\Delta_T = 5 \times 10^{-5}$ eV at $d = 8$ QLs are taken from Ref. 29.

The aforementioned characteristics of the pairing with hybridization are shown in Fig. 6 for these four examples of Bi_2Se_3 films at $\varepsilon_1 = \varepsilon_3 = 1$. The gap calculated with hybridization is several orders of magnitude larger than the BCS gap. In the cases of strong hybridization at small d [Figs. 6(a) and 6(b)], the increase of the total gap above the pure hybridization gap Δ_T, being negligible compared with Δ_T itself and occurring in a range of several thousands Kelvins, can hardly be observed. However, when the hybridization is

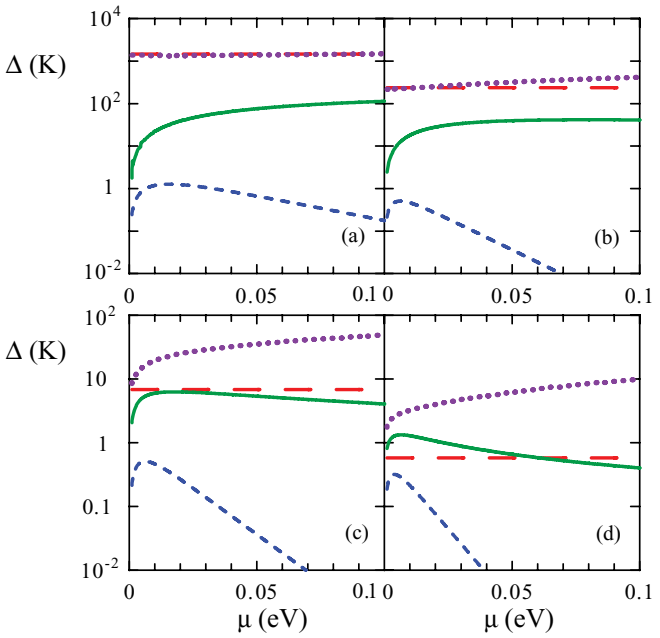

FIG. 6. (Color online) Characteristics of the pairing in suspended Bi_2Se_3 films with hybridization: the increase $\Delta_0 - \Delta_T$ of the total gap (solid line) above the hybridization gap Δ_T (long-dashed line), the characteristic temperature range $T_{\rm char}$ (dotted line) at which the gap increases, and the BCS gap $\Delta_0^{\rm BCS}$ (short-dashed line) calculated without hybridization. The data on hybridization are taken from Ref. 25 for (a) $d = 2$ QLs and (b) $d = 5$ QLs and from Ref. 29 for (c) $d = 5$ QLs and (d) $d = 8$ QLs.

rather weak [Figs. 6(c) and 6(d)], the gap can grow significantly (up to several times) when we lower the temperature by several tens of Kelvins. In this case the gap itself is not larger than several Kelvins.

We can conclude that the temperature-dependent growth of the total gap is appreciable only if the hybridization is sufficiently weak, i.e., in moderately thin films. Since the gap itself becomes too small in thicker films, the optimal thickness for observing the pairing is about 5–8 QLs.

IV. INFLUENCE OF DISORDER

As is known, charged impurities suppress the electron-hole pairing in two-layer systems[45,52,57] since they, being usually uncorrelated in two layers, break the Cooper pairs by differently scattering two pair constituents. According to the Abrikosov-Gor'kov theory, applied to the case of electron-hole pairing, the Gor'kov equations remain the same as in the case of a clean system but with Matsubara frequencies ω_n and gaps at these frequencies Δ_n renormalized in the following way:

$$\omega_n \to \tilde{\omega}_n = \omega_n + (\gamma_{11} + \gamma_{22}) \frac{\tilde{\omega}_n}{\sqrt{\tilde{\omega}_n^2 + \tilde{\Delta}_n^2}},$$
$$\Delta_n \to \tilde{\Delta}_n = \Delta - 2\gamma_{12} \frac{\tilde{\Delta}_n}{\sqrt{\tilde{\omega}_n^2 + \tilde{\Delta}_n^2}}, \tag{10}$$

where $\omega_n = \pi T(2n+1)$ and Δ are the initial Mathubara frequencies and gap, respectively. The quantities γ_{ij} correspond to intralayer (γ_{11} and γ_{22} for top and bottom surfaces, respectively) and interlayer (γ_{12}) correlation functions of the random impurity potential.

The gap Eq. (9) for the disordered system takes the form

$$\Delta = \Delta_T + \lambda T \sum_{n=-\infty}^{+\infty} \int_{-w}^{w} d\xi \frac{\tilde{\Delta}_n}{\tilde{\omega}_n^2 + \xi^2 + \tilde{\Delta}_n^2}. \tag{11}$$

When $\gamma_{11} + \gamma_{22} + 2\gamma_{12} = 0$, the impurities do not affect the result of the energy integration and frequency summation in Eq. (11), and thus, the pairing characteristics remain the same. In superconductors it corresponds to the case of nonmagnetic impurities which, according to the Anderson theorem, do not suppress the pairing. In a two-layer system, this situation requires perfect anticorrelation of the impurity potential between the layers and thus is hardly realizable in practice.

In reality, when the range of the impurity potential significantly exceeds the film thickness (the limit $d \to 0$) and both surfaces of the film are equally disordered, we have $\gamma_{11} = \gamma_{22} = \gamma_{12} = 2\gamma$, where γ is the electron-damping rate. For further calculations, we consider the opposite case of short-range impurities and relatively thick films ($d \to \infty$) when $\gamma_{11} = \gamma_{22} = 2\gamma$ and $\gamma_{12} = 0$.

We can estimate γ on the basis of the data on the surface-carrier mobilities μ_c, determining the surface conductivity of a TI, expressed through the Drude formula

$$\sigma = ne\mu_c = \frac{e^2\mu}{4\pi\gamma}, \tag{12}$$

where $n = \mu^2/4\pi v_F^2$ is the surface-carrier concentration. In experiments on surface transport on Bi_2Se_3 (see the references cited in the review by Qi *et al.*),[2] the measured mobilities vary from ~100 to ~20 000 $\rm cm^2/V\,s$. For calculations, we choose the example of a dirty sample where $\mu_c = 500\ \rm cm^2/V\,s$ and the example of a clean sample with $\mu_c = 10^4\ \rm cm^2/V\,s$.

In the usual Abrikosov-Gor'kov theory, the pair-breaking disorder reduces both the gap and critical temperature, and sufficiently strong disorder can suppress the pairing completely. In our case the total gap Δ is always larger than the hybridization gap Δ_T. However, in the presence of disorder, their difference $\Delta - \Delta_T$ diminishes in comparison with that in a clean system.

In Fig. 7 the increase of the gap $\Delta_0 - \Delta_T$ calculated numerically from Eqs. (10) and (11) is plotted at different disorder strengths for different examples of suspended Bi_2Se_3 films. It is seen that disorder rather weakly affects the pairing at strong hybridization [Fig. 7(a)] since the gap is very large in this case. At weak hybridization, when the effect of the pairing on the gap is expected to be most pronounced, even moderate disorder drastically reduces $\Delta_0 - \Delta_T$ [Figs. 7(c) and 7(d)]. Therefore, we can conclude that the temperature-dependent increase of the gap due to the pairing can be observed only in very clean (with carrier mobilities $\mu_c > 10^4\ \rm cm^2/V\,s$) and moderately thin (5–8 QLs) TI films.

V. SUPPRESSION OF SCREENING

In the previous sections we have considered the pairing potential screened by a dielectric environment and by metallic electron and hole gases on two surfaces of the film. However, this consideration is not completely self-consistent since the

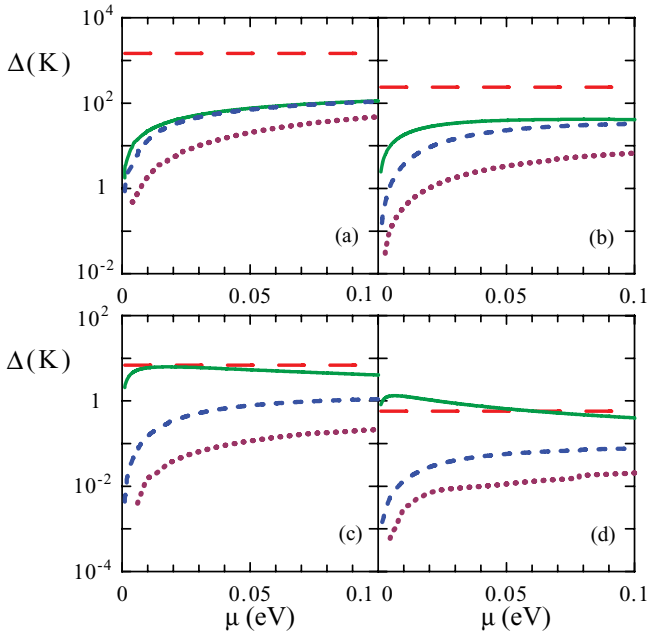

FIG. 7. (Color online) The increase $\Delta_0 - \Delta_T$ of the zero-temperature total gap above the hybridization gap with no disorder (solid line), at $\mu_c = 10^4$ cm^2/V s (short-dashed line), and at $\mu_c = 500$ cm^2/V s (dotted line). The hybridization gap (long-dashed line) in Bi_2Se_3 films is taken from Ref. 25 for (a) $d = 2$ QLs and (b) $d = 5$ QLs and from Ref. 29 for (c) $d = 5$ QLs and (d) $d = 8$ QLs.

film becomes insulating on the surface due to the appearance of the gap in the spectrum. When the gap is very large (especially in the case of strong hybridization), the screening by electron and hole gases can substantially differ from that in a metallic system. In this case we should take into account self-consistent weakening of the screening caused by the pairing. (A similar effect was considered earlier for semiconductor quantum wells[46] and graphene bilayers.[41,58])

When the gap Δ appears in the system due to interlayer pairing or hybridization, the intralayer static polarizabilities Π_{11} and Π_{22} are no longer equal to the intrinsic polarizability Π_0 and can be expressed in the RPA as (see Refs. 41 and 58)

$$\Pi_{11,22}(q) = -g\sum_{\gamma\gamma'}\int \frac{d\mathbf{p}}{(2\pi)^2}\frac{1+\gamma\gamma'\cos(\varphi-\varphi')}{2} \times\left(\frac{u^2_{p\gamma}v^2_{p'\gamma'}+v^2_{p\gamma}u^2_{p'\gamma'}}{E_{p\gamma}+E_{p\gamma'}}\right), \quad (13)$$

where $\mathbf{p}' = \mathbf{p}+\mathbf{q}$; φ and φ' are azimuthal angles of the momenta $\mathbf{p}$ and $\mathbf{p}'$, respectively; $\gamma,\gamma' = \pm 1$ are indices denoting the conduction $(+1)$ and valence (-1) bands (i.e., the upper and lower parts of the double Dirac cone); and $E_{p\gamma} = \sqrt{(\gamma v_F p-\mu)^2+\Delta^2}$ is the energy of the Bogolyubov excitation in the band γ. The coherence factors $u_{p\gamma}$ and $v_{p\gamma}$ are positive and determined by the equations

$$u^2_{p\gamma} = \frac{1}{2}+\frac{\gamma v_F p-\mu}{2E_{p\gamma}}, \quad v^2_{p\gamma} = \frac{1}{2}-\frac{\gamma v_F p-\mu}{2E_{p\gamma}}. \quad (14)$$

In a two-layer system, interlayer pairing or hybridization also leads to the appearance of the anomalous polarizability Π_{12} describing the direct response of the charge density in one layer to an electric field in the other layer. In the RPA, it can be calculated as

$$\Pi_{12}(q) = g\sum_{\gamma\gamma'}\int \frac{d\mathbf{p}}{(2\pi)^2}\frac{1+\gamma\gamma'\cos(\varphi-\varphi')}{2} \times\left(\frac{2u_{p\gamma}v_{p\gamma}u_{p'\gamma'}v_{p'\gamma'}}{E_{p\gamma}+E_{p\gamma'}}\right). \quad (15)$$

We performed a numerical solving of the gap Eq. (9), taking into account hybridization and with the pairing potential of Eqs. (1) and (2) self-consistently screened by electrons and holes with the polarizabilities of Eqs. (13) and (15). In this case the usual BCS method of Eq. (5), which reduces the pairing potential to a single coupling constant λ on the Fermi surface, is inapplicable since the integral in Eq. (8) diverges due to the absence of long-range screening in the gapped system. Thus, we perform full integration of Eq. (4) over momentum $\mathbf{p}'$ in the region $|v_F p'-\mu| < w$, where $\Delta(\mathbf{p}') \neq 0$.

Our calculations show that at sufficiently weak coupling the gap is several times larger than in the case of metallic screening. At stronger coupling, two additional solutions of the gap equation appear that are several orders of magnitude larger than the small gap that exists at weak coupling. Only the maximal of the resulting three gaps, providing the lowest ground-state energy, will be established in the system. With a further increase of the coupling (say, a decrease of $p_F d$), the two smallest solutions disappear, and only one large gap remains (see the inset in Fig. 8).

In Fig. 8 we show the phase diagram of a Bi_2Se_3 film at $T = 0$ with self-consistent weakening of the screening but without hybridization. At nonzero hybridization, the regions of one large gap and of three solutions in this diagram would grow in size. At nonzero temperature the smallest gap gradually vanishes at small critical temperature (as in the usual BCS model), but the two largest gaps disappear at much larger

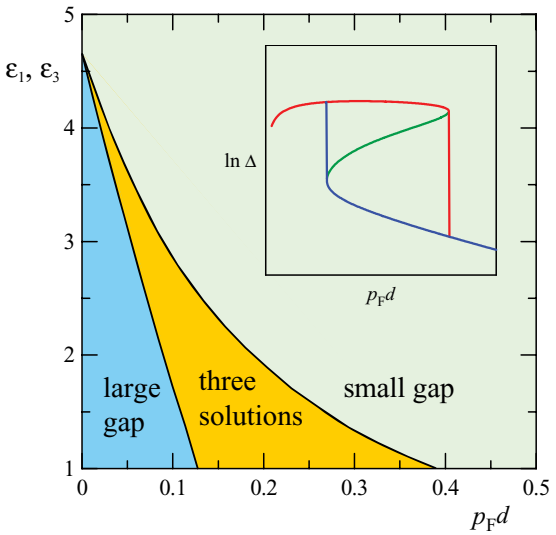

FIG. 8. (Color online) Phase diagram of the pairing (without hybridization) in a Bi_2Se_3 film at different dielectric constants of the surrounding medium $\varepsilon_1 = \varepsilon_3$ and different dimensionless thicknesses $p_F d$. The regions when the gap equation at $T = 0$ gives one small gap, three gaps, and one large gap are shown. Inset: Typical behavior of solutions Δ of the gap equation at $\varepsilon_1, \varepsilon_3 < 4.5$.

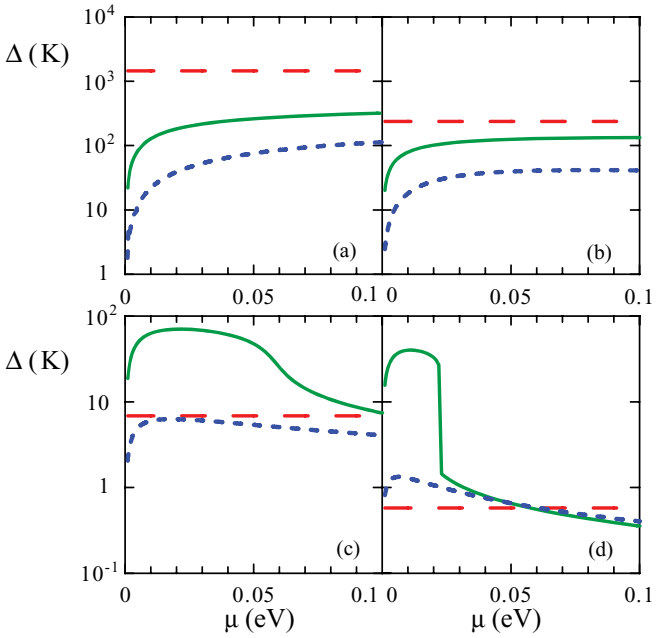

FIG. 9. (Color online) The increase $\Delta_0 - \Delta_T$ of the zero-temperature total gap in suspended Bi_2Se_3 films above the hybridization gap with (solid line) and without (short-dashed line) taking into account self-consistent suppression of the screening. The hybridization gap (long-dashed line) in Bi_2Se_3 films is taken from Ref. 25 for (a) $d = 2$ QLs and (b) $d = 5$ QLs and from Ref. 29 for (c) $d = 5$ QLs and (d) $d = 8$ QLs.

temperature, transitioning abruptly from nonzero values to zero, characteristic to the first-order phase transition. (This fact was also noted in Ref. 41.)

In Fig. 9 we demonstrate that $\Delta_0 - \Delta_T$ becomes larger by several times at strong hybridization [Figs. 9(a) and 9(b)] and by an order of magnitude at weaker hybridization [Figs. 9(c) and 9(d)] in comparison with the results obtained with metallic screening. Our predictions for observability of the pairing become more optimistic when we treat the screening self-consistently, especially for relatively thick films with weak hybridization where even a sharp transition to a strongly correlated state can occur [Fig. 9(d)].

VI. CONCLUSIONS

We have considered the pairing of spatially separated massless Dirac electrons and holes created on opposite surfaces of a TI thin film by antisymmetric doping. The main advantage of such a system over a two-layer graphene system is the fourfold smaller degeneracy of the electron states leading to much weaker screening and much larger coupling constants. The effect of a large bulk dielectric constant of the TI itself on the pairing can be negligible when the film is sufficiently thin.

Our calculations with the BCS approximation show that the pairing gap is large enough to be observable when the film thickness is less than 15 nm. In this case, however, tunneling between opposite surfaces leads to the hybridization of electron and hole states. Such hybridization, on the one hand, effectively increases the gap. On the other hand, the pairing can become hardly observable on a background of strong hybridization.

We show that the pairing causes an increase of the total gap in the spectrum above the pure hybridization gap when the temperature is decreased. This effect can be observed only in moderately thin films (about 5–8 QLs for Bi_2Se_3) where the hybridization is rather weak and the effect of the pairing is noticeable on its background. Another way to observe the pairing can be based on measuring the change of the gap with varying surface-electron and -hole chemical potentials. Charged impurities and other disorder on surfaces of the film suppress the pairing, so it can be observed only in sufficiently clean TIs. (Surface-carrier mobility should be at least 10^4 cm^2/V s.)

Also, we have demonstrated that the BCS approximation, by assuming the metallic screening with surface carriers, underestimates the coupling strength since the real screening in the gapped system is much weaker. The self-consistent treatment of the screening demonstrates that the gap can be orders of magnitude larger than that given by the BCS model, and observation of the pairing in TI films can turn out to be more feasible. Multiband and dynamical effects can additionally increase the gap.

The realization of electron-hole pairing in a TI thin film is a difficult task, including chemical doping of the bulk TI to an insulating state and, at the same time, doping of two opposite surfaces to electron- and hole-metallic states by means of gate electrodes or charged impurities. Another challenge is the fabrication of separate contacts to the surfaces. However, considerable progress achieved recently in experimental studies of TIs and TI thin films (see Refs. 1,2 and the references therein) gives hope that conditions suitable for electron-hole pairing can be reached in coming years. In particular, transport measurements in a regime of coexistence of electrons and holes on opposite surfaces of a Bi_2Se_3 film were carried out in Ref. 63.

In this article, we considered only the manifestation of the pairing in the temperature dependence of the gap in the spectrum. For an exciton condensate in electron-hole bilayers, such signatures as dipolar superfluidity,[44] Josephson-like effects,[44,47,64,65] peculiarities of the drag effect,[39,66,67] and anomalous electromagnetic responses[68,69] have been predicted. Strong hybridization occurring in TI thin films imposes serious limitations on the observability of these phenomena. As is known, tunneling in the electron-hole bilayer leads to the fixation of the condensate phase and to the absence of uniform dipolar superfluidity. However, the superfluidity can arise locally in the form of Josephson-like vortices[64,65] or a vortex lattice.[47] In the latter case, the dipolar current flowing along the bilayer should exceed some critical value in order for the vortex lattice to be stable. At high enough temperatures, the vortex lattice undergoes a dislocation-mediated melting when pairs of edge dislocations dissociate and proliferate (see Ref. 47). It is interesting to note that dislocation ends in this case are topologically equivalent to vortices in a superfluid condensate and thus can settle Majorana zero-energy modes,[34] which can be manipulated for the purpose of quantum computations.

ACKNOWLEDGMENTS

The work was supported by the Russian Foundation for Basic Research. D.K.E. and A.A.S. were also supported by the Dynasty Foundation and by a grant of the President of the Russian Federation for Young Scientists (No. MK-5288.2011.2).

*lozovik@isan.troitsk.ru
†aasokolik@yandex.ru

[1] M. Z. Hasan and C. L. Kane, Rev. Mod. Phys. **82**, 3045 (2010).
[2] X.-L. Qi and S.-C. Zhang, Rev. Mod. Phys. **83**, 1057 (2011).
[3] H. Zhang, C.-X. Liu, X.-L. Qi, X. Dai, Z. Fang, and S.-C. Zhang, Nat. Phys. **5**, 438 (2009).
[4] D. Hsieh, Y. Xia, L. Wray, D. Qian, A. Pal, J. H. Dil, J. Osterwalder, F. Meier, G. Bihlmayer, C. L. Kane, Y. S. Hor, R. J. Cava, and M. Z. Hasan, Science **323**, 919 (2009).
[5] Y. L. Chen, J. G. Analytis, Z. H. Chu, Z. K. Liu, S. K. Mo, X. L. Qi, H. J. Zhang, D. H. Lu, X. Dai, Z. Fang, S. C. Zhang, I. R. Fisher, Z. Hussain, and Z. X. Shen, Science **325**, 178 (2009).
[6] Y. Xia, L. Wray, D. Qian, D. Hsieh, A. Pal, H. Lin, A. Bansil, D. Grauer, Y. Hor, R. Cava, and M. Z. Hasan, Nat. Phys. **5**, 398 (2009).
[7] A. H. Castro Neto, F. Guinea, N. M. R. Peres, K. S. Novoselov, and A. K. Geim, Rev. Mod. Phys. **81**, 109 (2009).
[8] Q. Liu, C.-X. Liu, C. Xu, X.-L. Qi, and S.-C. Zhang, Phys. Rev. Lett. **102**, 156603 (2009).
[9] Y. L. Chen, J.-H. Chu, J. G. Analytis, Z. K. Liu, K. Igarashi, H.-H. Kuo, X. L. Qi, S. K. Mo, R. G. Moore, D. H. Lu, M. Hashimoto, T. Sasagawa, S. C. Zhang, I. R. Fisher, Z. Hussain, and Z. X. Shen, Science **329**, 659 (2010).
[10] X. L. Qi, T. L. Hughes, and S. C. Zhang, Phys. Rev. B **78**, 195424 (2008).
[11] A. M. Essin, J. E. Moore, and D. Vanderbilt, Phys. Rev. Lett. **102**, 146805 (2009).
[12] L. Fu and C. L. Kane, Phys. Rev. Lett. **100**, 096407 (2008).
[13] Y. S. Hor, A. J. Williams, J. G. Checkelsky, P. Roushan, J. Seo, Q. Xu, H. W. Zandbergen, A. Yazdani, N. P. Ong, and R. J. Cava, Phys. Rev. Lett. **104**, 057001 (2010).
[14] C.-K. Lu and I. F. Herbut, Phys. Rev. B **82**, 144505 (2010).
[15] M. C. Diamantini, P. Sodano, and C. A. Trugenberger, New J. Phys. **14**, 063013 (2012).
[16] G. Zhang, H. Qin, J. Teng, J. Guo, Q. Guo, X. Dai, Z. Fang, and K. Wu, Appl. Phys. Lett. **95**, 053114 (2009).
[17] H. D. Li, Z. Y. Wang, X. Kan, X. Guo, H. T. He, Z. Wang, J. N. Wang, T. L. Wong, N. Wang, and M. H. Xie, New J. Phys. **12**, 103038 (2010).
[18] Y.-Y. Li, G. Wang, X.-G. Zhu, M.-H. Liu, C. Ye, X. Chen, Y.-Y. Wang, K. He, L.-L. Wang, X.-C. Ma, H.-J. Zhang, X. Dai, Z. Fang, X.-C. Xie, Y. Liu, X.-L. Qi, J.-F. Jia, S.-C. Zhang, and Q.-K. Xue, Adv. Mater. (Weinheim, Ger.) **22**, 4002 (2010).
[19] N. Bansal, Y. S. Kim, E. Edrey, M. Brahlek, Y. Horibe, K. Iida, M. Tanimura, G.-H. Li, T. Feng, H.-D. Lee, T. Gustafsson, E. Andrei, and S. Oh, Thin Solid Films **520**, 224 (2010).
[20] D. Kong, W. Dang, J. J. Cha, H. Li, S. Meister, H. Peng, Z. Liu, and Y. Cui, Nano Lett. **10**, 2245 (2010).
[21] S. S. Hong, W. Kundhikanjana, J. J. Cha, K. Lai, D. Kong, S. Meister, M. A. Kelly, Z.-X. Shen, and Y. Cui, Nano Lett. **10**, 3118 (2010).
[22] K. M. F. Shahil, M. Z. Hossain, D. Teweldebrhan, and A. A. Balandin, Appl. Phys. Lett. **96**, 153103 (2010).
[23] D. Teweldebrhan, V. Goyal, and A. A. Balandin, Nano Lett. **10**, 1209 (2010).
[24] J. Linder, T. Yokoyama, and A. Sudbo, Phys. Rev. B **80**, 205401 (2009).
[25] Y. Zhang, K. He, C.-Z. Chang, C.-L. Song, L.-L. Wang, X. Chen, J.-F. Jia, Z. Fang, X. Dai, W.-Y. Shan, S.-Q. Shen, Q. Niu, X.-L. Qi, S.-C. Zhang, X.-C. Ma, and Q.-K. Xue, Nat. Phys. **6**, 584 (2010).
[26] Y. Sakamoto, T. Hirahara, H. Miyazaki, S. I. Kimura, and S. Hasegawa, Phys. Rev. B **81**, 165432 (2010).
[27] G. Wang, X. Zhu, J. Wen, X. Chen, K. He, L. Wang, X. Ma, Y. Liu, X. Dai, Z. Fang, J. Jia, and Q. Xue, Nano Res. **3**, 874 (2010).
[28] K. Park, J. J. Heremans, V. W. Scarola, and D. Minic, Phys. Rev. Lett. **105**, 186801 (2010).
[29] K. Ebihara, K. Yada, A. Yamakage, and Y. Tanaka, Physica E (Amsterdam, Neth.) **44**, 885 (2012).
[30] H.-Z. Lu, W.-Y. Shan, W. Yao, Q. Niu, and S.-Q. Shen, Phys. Rev. B **81**, 115407 (2010).
[31] X. Zhang, J. Wang, and S.-C. Zhang, Phys. Rev. B **82**, 245107 (2010).
[32] Z. Yang and J. H. Han, Phys. Rev. B **83**, 045415 (2011).
[33] A. A. Zyuzin and A. A. Burkov, Phys. Rev. B **83**, 195413 (2011).
[34] B. Seradjeh, J. E. Moore, and M. Franz, Phys. Rev. Lett. **103**, 066402 (2009).
[35] N. Hao, P. Zhang, and Y. Wang, Phys. Rev. B **84**, 155447 (2011).
[36] G. Y. Cho and J. E. Moore, Phys. Rev. B **84**, 165101 (2011).
[37] D. Tilahun, B. Lee, E. M. Hankiewicz, and A. H. MacDonald, Phys. Rev. Lett. **107**, 246401 (2011).
[38] Z. Wang, N. Hao, Z.-G. Fu, and P. Zhang, New J. Phys. **14**, 063010 (2012).
[39] M. P. Mink, H. T. C. Stoof, R. A. Duine, M. Polini, and G. Vignale, Phys. Rev. Lett. **108**, 186402 (2012).
[40] E. G. Moon and C. Xu, Europhys. Lett. **97**, 66008 (2012).
[41] I. Sodemann, D. A. Pesin, and A. H. MacDonald, Phys. Rev. B **85**, 195136 (2012).
[42] B. Seradjeh, Phys. Rev. B **86**, 121101(R) (2008).
[43] B. Seradjeh, Phys. Rev. B **85**, 235146 (2012).
[44] Yu. E. Lozovik and V. I. Yudson, Pis'ma Zh. Eksp. Teor. Fiz. **22**, 556 (1975) [JETP Lett. **22**, 274 (1975)]; Zh. Eksp. Teor. Fiz. **71**, 738 (1976) [Sov. Phys. JETP **44**, 389 (1976)].
[45] Yu. E. Lozovik and V. I. Yudson, Solid State Commun. **21**, 211 (1977).
[46] Yu. E. Lozovik and O. L. Berman, Zh. Eksp. Teor. Fiz. **111**, 1879 (1997) [JETP **84**, 1027 (1997)].
[47] S. I. Shevchenko, Phys. Rev. Lett. **72**, 3242 (1994).
[48] R. Dillenschneider and J. H. Han, Phys. Rev. B **78**, 045401 (2008).
[49] Yu. E. Lozovik and A. A. Sokolik, Pis'ma Zh. Eksp. Teor. Fiz. **87**, 61 (2008) [JETP Lett. **87**, 55 (2008)].
[50] H. Min, R. Bistritzer, J.-J. Su, and A. H. MacDonald, Phys. Rev. B **78**, 121401(R) (2008).
[51] C.-H. Zhang and Y. N. Joglekar, Phys. Rev. B **77**, 233405 (2008).
[52] R. Bistritzer and A. H. MacDonald, Phys. Rev. Lett. **101**, 256406 (2008).
[53] M. Y. Kharitonov and K. B. Efetov, Phys. Rev. B **78**, 241401(R) (2008); Semicond. Sci. Technol. **25**, 034004 (2010).
[54] Yu. E. Lozovik and A. A. Sokolik, Phys. Lett. A **374**, 326 (2009); Eur. Phys. J. B **73**, 195 (2009).
[55] Yu. E. Lozovik, S. L. Ogarkov, and A. A. Sokolik, Philos. Trans. R. Soc., A **368**, 5417 (2010).
[56] M. P. Mink, H. T. C. Stoof, R. A. Duine, and A. H. MacDonald, Phys. Rev. B **84**, 155409 (2011).
[57] D. K. Efimkin, V. A. Kulbachinskii, and Yu. E. Lozovik, Pis'ma Zh. Eksp. Teor. Fiz. **93**, 238 (2011) [JETP Lett. **93**, 219 (2011)].
[58] Yu. E. Lozovik, S. L. Ogarkov, and A. A. Sokolik, Phys. Rev. B **86**, 045429 (2012).

[59] B. Wunsch, T. Stauber, F. Sols, and F. Guinea, New J. Phys. **8**, 318 (2006).

[60] E. H. Hwang and S. Das Sarma, Phys. Rev. B **75**, 205418 (2007).

[61] *Bismuth Selenide (Bi2Se3) Optical Properties, Dielectric Constants*, edited by O. Madelung, U. Rossler, and M. Schulz, Landolt-Börnstein New Series, Group III, Vol. 41C (Springer-Verlag, Berlin, 1998).

[62] *Bismuth Telluride (Bi2Te3) Optical Properties, Dielectric Constant*, edited by O. Madelung, U. Rossler, and M. Schulz, Landolt-Börnstein New Series, Group III, Vol. 41C (Springer-Verlag, Berlin, 1998).

[63] J. Chen, X. Y. He, K. H. Wu, Z. Q. Ji, L. Lu, J. R. Shi, J. H. Smet, and Y. Q. Li, Phys. Rev. B **83**, 241304(R) (2011).

[64] A. V. Klyuchnik and Yu. E. Lozovik, Zh. Eksp. Teor. Fiz. **76**, 670 (1978) [Sov. Phys. JETP **49**, 335 (1978)].

[65] Yu. E. Lozovik and A. V. Poushnov, Phys. Lett. A **228**, 399 (1997).

[66] S. Conti, G. Vignale, and A. H. MacDonald, Phys. Rev. B **57**, R6846 (1998).

[67] B. Y.-K. Hu, Phys. Rev. Lett. **85**, 820 (2000).

[68] Yu. E. Lozovik and I. V. Ovchinnikov, Phys. Rev. B **66**, 075124 (2002).

[69] A. V. Balatsky, Y. N. Joglekar, and P. B. Littlewood, Phys. Rev. Lett. **93**, 266801 (2004).